

# Coulomb drag as a probe of quantum Hall systems

Felix von Oppen<sup>1,2</sup>, I.V. Gornyi<sup>3,\*</sup>, and A.D. Mirlin<sup>3,4,\*\*</sup>

<sup>1</sup> Institut für Theoretische Physik, Freie Universität Berlin, 14195 Berlin, Germany

<sup>2</sup> Dept. of Condensed Matter Physics, Weizmann Institute of Science, Rehovot, Israel

<sup>3</sup> Institut für Nanotechnologie, Forschungszentrum Karlsruhe, 76021 Karlsruhe, Germany

<sup>4</sup> Institut für Theorie der Kondensierten Materie, Universität Karlsruhe, 76128 Karlsruhe, Germany

**Abstract.** Experiments on Coulomb drag in double-layer systems in the quantum-Hall regime have observed a number of surprises which were only partially understood for some time. The most striking observations are that Coulomb drag can become negative in the regime of high Landau levels and that its temperature dependence is non-monotonous. In this contribution, we review a theory of Coulomb drag in high Landau levels for the ballistic regime which is in good agreement with the experiments. Our starting point is the diagrammatic approach to drag, treating the interlayer interaction perturbatively and accounting for disorder within the self-consistent Born approximation. Our theory shows that drag in high Landau levels is an interplay of two contributions arising from different sources for particle-hole asymmetry, namely the curvature of the zero-field electron dispersion and the Landau-level density of states.

Frictional drag [1,2] between two parallel two-dimensional electron systems has become a powerful tool to study quantum Hall systems. When a current  $I$  is applied to one (active) layer, interlayer interactions will impart momentum to the carriers of the second, passive layer. If no current is allowed to flow in the passive layer, a voltage  $V$  builds up there, neutralizing the momentum transfer. The ratio  $V/I$  is known as drag resistance or transresistance. Depending on the strength of the interlayer interaction – tunable in experiment by the interlayer distance – one can distinguish between two regimes. At large separation, the interlayer interaction can be treated perturbatively. When the two layers are brought closer together, the interlayer interaction can become strong enough to lead to the formation of states with *interlayer* correlations. In this paper, we will be concerned with the first regime of weak interlayer interaction.

The picture of momentum transfer between the two layers leads to the following basic predictions. Clearly, the momentum transfer is independent

---

\* Also at A.F. Ioffe Physico-Technical Institute, 194021 St. Petersburg, Russia.

\*\* Also at Petersburg Nuclear Physics Institute, 188350 St. Petersburg, Russia.

of the nature (electrons or holes) of the carriers in the two layers. Thus, one expects that the sign of the drag resistance depends on the relative sign of the carriers in the two layers. Conventionally, one refers to the resulting drag between two layers with equal (opposite) carriers as positive (negative). A consequence of this is that drag vanishes for particle-hole symmetric systems. In addition, drag is expected to increase monotonously with temperature due to the increased phase space for interlayer scattering. These basic expectations were well supported by early theoretical considerations of Zheng and MacDonald [3].

## 1 Coulomb drag in high Landau levels

Remarkably, a series of experiments [4–6] on drag in quantum Hall systems shows that these simple expectations are violated in the regime of high Landau levels (large filling factor). First experiments [4,5] showed that drag can change sign as function of magnetic field or filling factor difference, when the two layers are at different densities. This was surprising because the carriers in both layers are electrons. A more recent experiment [6] studied the temperature dependence and found that while exhibiting the expected increase with temperature at high temperatures, an additional peak develops at low temperatures which can be either positive or negative, depending on the filling factor difference between the two layers. This non-monotonous temperature dependence contrasts with the phase-space argument given above.

Drawing an analogy between partially filled Landau levels and partially filled Bloch bands, it is natural to suggest [4] that a less-than-half-filled Landau level behaves as an electron-like band while a more than half-filled Landau level behaves as a hole-like band. This analogy suggests that there are sign changes in the drag resistivity as function of the filling factor difference between the two layers. While there is an element of truth in this picture, it turns out [7] that this analogy can be rather misleading. One reason is that it neglects the contributions to the drag resistivity which arise from the Hall conductivity.

We find [8] from a careful evaluation of the diagrammatic expressions for the drag conductivity that the experiments can be understood in terms of the interplay of two contributions which are associated with two sources of particle-hole symmetry violation. One source is the curvature of the (quadratic) zero-magnetic-field dispersion of the electrons. This contribution is closely related to the conventional picture for drag described above. Thus, this contribution which dominates at high temperatures, indeed increases monotonously with temperature and has a fixed sign (positive for two electron layers). A second source is related to the oscillatory Landau-level density of states. This anomalous contribution dominates at low temperatures where it exhibits a peak. Its sign depends on the filling factor difference between the two layers. In the ballistic regime  $R_c \gg d$  ( $R_c$  denotes the cyclotron radius and  $d$  the

spacing between the two layers), the sign turns out to be in agreement with experiment.

## 2 Previous theoretical work

We briefly discuss previous theoretical work. Early theoretical work [9] on Coulomb drag in a magnetic field in the limit of high Landau levels showed that the magnetic field strongly enhances the Coulomb drag. More recent work [7] showed that Landau-level quantization can lead to sign changes in drag. However, the results obtained for the diffusive regime indicated that unlike the experimental observation, negative drag should be observed for equal filling factors in the two layers. None of these works can explain the observed non-monotonic temperature dependence.

Ref. [7] started from an alternative picture for the drag *conductivity* which can be roughly thought of as follows. The fluctuations of the electron density of the active layer lead to a fluctuating electric potential which is seen by the passive layer. Due to the applied voltage in the active layer, these electric potential fluctuations are not fully isotropic in the wavevector  $\mathbf{q}$  and thus induce a *dc* current in the passive layer in nonlinear response. This argument shows that drag is related to the "nonlinear susceptibility"  $\mathbf{\Gamma}(\mathbf{q}, \omega)$  which, *loosely speaking*, gives the *dc* current response to an electric potential  $\phi(\mathbf{q}, \omega)$  in quadratic order,  $\mathbf{j}_{dc} = \mathbf{\Gamma}(\mathbf{q}, \omega)|\phi(\mathbf{q}, \omega)|^2$ . (A more accurate, diagrammatic definition is given in the next section.) The diagrammatic approach (see below) shows that the anisotropic part of the electric potential fluctuations of the active layer is also related to  $\mathbf{\Gamma}(\mathbf{q}, \omega)$  of the active layer. As a result, one finds for the *dc* drag conductivity the expression [10,11]

$$\sigma_{ij}^{(D)} = \frac{e^2}{16\pi TS} \sum_{\mathbf{q}} \int_{-\infty}^{\infty} \frac{d\omega}{\sinh^2(\omega/2T)} \Gamma_i^{(1)}(\mathbf{q}, \omega) \Gamma_j^{(2)}(\mathbf{q}, \omega) |U(\mathbf{q}, \omega)|^2. \quad (1)$$

where  $S$  denotes the area of the sample,  $T$  the temperature, and  $U(\mathbf{q}, \omega)$  the screened interlayer interaction.

In the limit in which the current response of the passive layer to the electric potential fluctuation generated by the active layer is local, one can argue [12,7] in an elementary fashion that the "nonlinear susceptibility" becomes

$$\mathbf{\Gamma}(\mathbf{q}, \omega) = 2 \frac{d\sigma}{d(en)} \cdot \mathbf{q} \text{Im} \Pi(\mathbf{q}, \omega), \quad (2)$$

where  $\Pi(\mathbf{q}, \omega)$  is the polarization operator of the layer,  $\sigma$  the conductivity tensor, and  $n$  denotes the electron density. Inserting this into the expression for the drag conductivity which is related to the experimentally measured drag resistivity by  $\rho_D = \rho^{(1)} \sigma^{(D)} \rho^{(2)}$  (here  $\rho^{(i)}$  denotes the resistivity of the  $i$ th layer), one finds [7] that the drag resistivity, takes the form

$$\rho^{(D)} \sim \rho^{(1)} \frac{d\sigma^{(1)}}{dn} \frac{d\sigma^{(2)}}{dn} \rho^{(2)}. \quad (3)$$

Here, the prefactor is positive. From this expression, we can read off the following results:

- Replacing the conductivity and resistivity tensors by their Drude form, assuming that the scattering time is independent of density, and using that in this case  $d\sigma/dn = \pm\sigma/n$  (the plus (minus) sign is valid for electrons (holes), respectively), we find that the drag resistivity is diagonal and its sign is in agreement with the simple arguments in the introduction to this paper.
- Even for the Drude conductivities, a density-dependent scattering time results in a finite Hall drag, i.e., an off-diagonal contribution to the drag resistivity.
- In the presence of a strong magnetic field, the longitudinal conductivity oscillates as a function of  $n$  due to the Shubnikov-deHaas oscillations. This leads to sign changes in the drag resistivity as function of the density difference between the layers.
- In strong magnetic fields, we have  $\rho_{xx} \ll \rho_{xy}$  and in addition, the self-consistent Born approximation (SCBA) valid in the limit of high Landau levels yields that  $d\sigma_{xx}/dn \gg d\sigma_{xy}/dn$ , so that to leading order

$$\rho_{xx}^{(D)} \sim \rho_{xy}^{(1)} \frac{d\sigma_{yy}^{(1)}}{dn} \frac{d\sigma_{yy}^{(2)}}{dn} \rho_{yx}^{(2)}. \quad (4)$$

Remarkably, since  $\rho_{xy} = -\rho_{yx}$ , this expression predicts that the drag resistivity is *negative* for *equal* densities. Thus, while the expression does exhibit sign oscillations as a function of filling factor differences between the two layers, the overall sign is in stark contrast to the experimentally observed positive sign for equal filling factors.

Thus, we have to go beyond the local, diffusive limit discussed in this section in order to understand the experiments. The corresponding diagrammatic calculation for the ballistic regime has recently been performed by us [8] and is sketched in the next section. We will see that this calculation resolves the discrepancy with experiment found here.

### 3 Diagrammatic theory

Our considerations [8] are based on the Kubo approach to Coulomb drag [10,11] which expresses the drag conductivity  $\sigma_{ij}^{(D)}(\mathbf{Q}, \Omega)$  in terms of a current-current correlation function,

$$\sigma_{ij}^{(D)}(\mathbf{Q}, \Omega) = \frac{1}{\Omega S} \int_0^\infty dt e^{i\Omega t} \left\langle [j_i^{(1)\dagger}(\mathbf{Q}, t), j_j^{(2)}(\mathbf{Q}, 0)] \right\rangle. \quad (5)$$

where  $i, j$  label the components of the drag conductivity tensor,  $\mathbf{Q}, \Omega$  denote the wave vector and frequency of the applied field,  $S$  is the area of the sample,

and  $j_i^{(l)}$  denotes the  $i$ th component of the current operator in the  $l$ th layer. The  $dc$  drag conductivity follows by taking the limit

$$\sigma_{ij}^{(D)} = \sigma_{ij}^{(D)}(\mathbf{Q} = 0, \Omega \rightarrow 0). \quad (6)$$

Considering the diagrams in Fig. 1, one obtains Eq. (1) for the  $dc$  drag conductivity [11,10]. The triangle vertex  $\Gamma(\mathbf{q}, \omega)$  takes the explicit form  $\Gamma = \Gamma^{(a)} + \Gamma^{(b)}$  with the two contributions

$$\begin{aligned} \Gamma^{(a)}(\mathbf{q}, \omega) = & \int \frac{d\epsilon}{4\pi i} \tanh \frac{\epsilon + \omega}{2T} \text{tr} \{ \mathbf{v} \mathcal{G}^+(\epsilon + \omega) e^{i\mathbf{q}\mathbf{r}} \mathcal{G}^+(\epsilon) e^{-i\mathbf{q}\mathbf{r}} \mathcal{G}^+(\epsilon + \omega) \\ & - \mathbf{v} \mathcal{G}^-(\epsilon + \omega) e^{i\mathbf{q}\mathbf{r}} \mathcal{G}^-(\epsilon) e^{-i\mathbf{q}\mathbf{r}} \mathcal{G}^-(\epsilon + \omega) \} + (\omega, \mathbf{q} \rightarrow -\omega, -\mathbf{q}) \end{aligned} \quad (7)$$

$$\begin{aligned} \Gamma^{(b)}(\mathbf{q}, \omega) = & \int \frac{d\epsilon}{4\pi i} (\tanh \frac{\epsilon + \omega}{2T} - \tanh \frac{\epsilon}{2T}) \\ & \times \text{tr} \{ \mathbf{v} \mathcal{G}^-(\epsilon + \omega) e^{i\mathbf{q}\mathbf{r}} [\mathcal{G}^-(\epsilon) - \mathcal{G}^+(\epsilon)] e^{-i\mathbf{q}\mathbf{r}} \mathcal{G}^+(\epsilon + \omega) \} \\ & + (\omega, \mathbf{q} \rightarrow -\omega, -\mathbf{q}) \end{aligned} \quad (8)$$

Here,  $\mathcal{G}^\pm(\epsilon)$  denotes the advanced/retarded Green function for a particular impurity configuration.

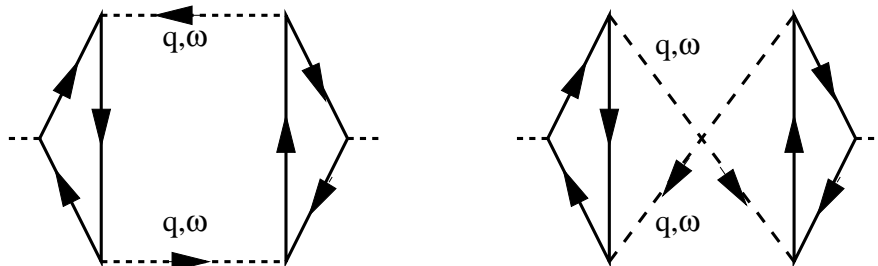


Fig. 1. Diagrams for the drag conductivity and for the triangle vertex  $\Gamma(\mathbf{q}, \omega)$

We perform the average over the white-noise impurity potential, characterized by  $\langle V(\mathbf{r}) \rangle = 0$  and  $\langle V(\mathbf{r})V(\mathbf{r}') \rangle = (1/2\pi\nu_0\tau_0)\delta(\mathbf{r} - \mathbf{r}')$ , within the self-consistent Born approximation (SCBA) [13]. ( $\nu_0$  and  $\tau_0$  denote the density of states and the elastic scattering time at zero magnetic field, respectively.) This approximation which neglects diagrams with crossing impurity lines, can be shown to give the leading contribution when the Fermi energy  $E_F$  is in a high LL with LL index  $N \gg 1$  [14].

### 3.1 The triangle vertex

In the ballistic regime for well-separated Landau levels, we can expand in three small parameters simultaneously. The parameter  $\Gamma/\hbar\omega_c \ll 1$  describes the fact that the LLs are well separated. Here  $\Gamma$  denotes the broadening of the

LL and  $\omega_c$  is the cyclotron frequency. The limit of high LLs allows us to treat  $1/N \ll 1$  as a small parameter. Finally, the ballistic regime is characterized by the small parameter  $1/qR_c \ll 1$ .

In the leading order in all three parameters, the following simplifications occur.

- There is no vertex correction due to disorder of the vector vertex in  $\mathbf{\Gamma}$ . This is actually generally true for white-noise disorder.
- There are also no vertex corrections of the scalar vertices due to the small parameter  $1/qR_c \ll 1$ .
- Two of the three Green function can be evaluated in the  $N$ th LL in which the Fermi energy resides. One Green function must be evaluated in a neighboring LL  $N \pm 1$  since the velocity operator, entering at the vector vertex, has nonzero matrix elements between neighboring LLs only.
- The matrix elements associated with the vertices can be evaluated in the semiclassical approximation due to  $N \gg 1$ .

Remarkably, at this order we find that there is an *exact cancellation* between the contributions  $\mathbf{\Gamma}^{(a)}$  and  $\mathbf{\Gamma}^{(b)}$ . This cancellation requires us to go beyond the leading order to find the relevant expression for the triangle vertex. Since all three small parameters are of comparable magnitude, we need to look for the leading correction in each of the three small parameters separately.

The leading correction in the ballistic parameter  $1/qR_c$  requires us to retain the vertex corrections to the scalar vertices. Within the SCBA, these vertex corrections arise from impurity ladders dressing both scalar vertices. As a result, we find

$$\mathbf{\Gamma}^{(1/qR_c)}(\mathbf{q}, \omega) = -\hat{\mathbf{q}} \frac{128\omega R_c}{\pi^2 \ell^2} \times \frac{(E - E_N)[\Gamma^2 - (E - E_N)^2]^{3/2}}{\Gamma^6} J_1(qR_c) J_0^3(qR_c). \quad (9)$$

Here, we introduced a superscript on  $\mathbf{\Gamma}(\mathbf{q}, \omega)$  in order to distinguish this contribution from other contributions computed below. Note that this is a purely longitudinal contribution to  $\mathbf{\Gamma}$  (i.e., parallel to  $\mathbf{q}$ ) which changes sign at the center of the LL.

Corrections of order  $\Gamma/\hbar\omega_c$  can arise from two sources:

- The Green functions adjacent to the current vertex are evaluated in Landau levels different from  $N$ . (Note that the Green function between the scalar vertices must still be evaluated in the  $N$ th Landau level because  $G_n^+ - G_n^- \sim \Gamma/(\hbar\omega_c)^2$  for  $n \neq N$ .)
- The diagrams giving the leading contribution can be evaluated more accurately, keeping corrections in  $\Gamma/\hbar\omega_c$ . Note that we may now neglect vertex corrections at the scalar vertices because we consider the leading order in  $qR_c \gg 1$ .

It turns out that the first contribution vanishes for both  $\Gamma^{(a)}$  and  $\Gamma^{(b)}$ . Considering the second contribution, it turns out that it still gives a vanishing contribution to the longitudinal triangle vertex, due to the cancellation between  $\Gamma^{(a)}$  and  $\Gamma^{(b)}$  described above. However, the transverse contribution to  $\Gamma^{(b)}$  no longer vanishes when considering corrections in  $\Gamma/\hbar\omega_c$ . In this way, we obtain the contribution

$$\begin{aligned} \Gamma^{(\Gamma/\hbar\omega_c)}(\mathbf{q}, \omega) &= -\hat{\mathbf{q}} \times \hat{\mathbf{z}} \frac{8\omega R_c}{\pi^2 \ell^2} \\ &\times \frac{(E - E_N)[\Gamma^2 - (E - E_N)^2]}{\omega_c \Gamma^4} J_0(qR_c) J_1(qR_c) \end{aligned} \quad (10)$$

to the triangle vertex. This is a transverse contribution to  $\Gamma$  which also changes sign in the center of the LL.

Finally, we consider the contribution to  $\Gamma$  due to terms of order  $q/k_F$  relative to the leading order. Such terms arise from a more accurate treatment of the matrix elements involved in the scalar vertices, keeping corrections of order  $1/N$  in the arguments of oscillatory terms. These corrections arise only for the contribution  $\Gamma^{(b)}$  and one finds

$$\Gamma^{(q/k_F)} = -\hat{\mathbf{z}} \times \mathbf{q} \frac{4\omega}{\pi^2} \frac{\Gamma^2 - (E - E_N)^2}{\Gamma^4} J_0^2(qR_c). \quad (11)$$

This expression can also be rewritten as

$$\Gamma^{(q/k_F)} = -\hat{\mathbf{z}} \times \mathbf{q} \frac{2\sigma_{xy}}{n} \text{Im} \Pi(\mathbf{q}, \omega) \quad (12)$$

with the polarization operator  $\Pi(\mathbf{q}, \omega)$  for the ballistic regime [cf. Eq. (15) below] and the Hall conductivity  $\sigma_{xy} = en_2/B - (e^2/\pi^2\hbar)N(\Gamma/\hbar\omega_c)[1 - (E - E_N)^2/\Gamma^2]^{3/2}$  in SCBA. This expression is a high-magnetic field analog of the conventional contribution to  $\Gamma$  [3] and thus does not change sign in the center of the LL.

### 3.2 Screened interlayer interaction

In this section, we briefly summarize the results for the screened interlayer interaction. For  $q$  small compared to the Thomas-Fermi screening wave vectors  $\kappa_{l,0} = 4\pi e^2 \nu_{l,0}$  ( $l = 1, 2$  labels the layer and  $\nu_{l,0}$  denotes the zero-field density of states per spin of layer  $l$ ), the screened interlayer interaction can be approximated as [11]

$$U(\mathbf{q}, \omega) \simeq \frac{\pi e^2 q}{\kappa_{1,0} \kappa_{2,0} \sinh(qd)} \frac{2\nu_{1,0}}{\Pi_1(\mathbf{q}, \omega)} \frac{2\nu_{2,0}}{\Pi_2(\mathbf{q}, \omega)}. \quad (13)$$

Here,  $d$  denotes the distance between the layers. The polarization operator of layer  $l$  is denoted by  $\Pi_l(\mathbf{q}, \omega)$ .

In the ballistic regime  $qR_c \ll 1$ , for  $\omega \ll \Gamma$ , the real part of the polarization operator takes the form

$$\text{Re}\Pi(\mathbf{q}, \omega) = 2\nu_0 + 2\nu(E)[J_0(qR_c)]^2. \quad (14)$$

Here, the second term arises from contributions of the  $N$ th LL, while the first term [15] arises from Landau levels  $n \neq N$ . The imaginary part of the polarization operator takes the form [16]

$$\text{Im}\Pi(\mathbf{q}, \omega) = 2\nu_0 \frac{2\omega\omega_c}{\pi\Gamma^2} \left[ 1 - \frac{(E - E_n)^2}{\Gamma^2} \right] [J_0(qR_c)]^2. \quad (15)$$

Note that  $\text{Im}\Pi \ll \text{Re}\Pi$ .

### 3.3 Results for the drag resistivity

In this section, we summarize our results for the drag resistivity based on the formalism sketched above [8]. In strong magnetic fields, the Hall conductivity  $\rho_{xy}$  dominates over  $\rho_{xx}$ . Therefore, using Eq. (1), the drag resistivity  $\rho_{xx}^{(D)} \simeq \rho_{xy}^{(1)} \sigma_{yy}^D \rho_{yx}^{(2)}$  can be expressed as

$$\begin{aligned} \rho_{xx}^D &= -\frac{B}{en_1} \frac{B}{en_2} \frac{1}{8\pi} \int_{-\infty}^{\infty} \frac{d\omega}{\sinh^2(\omega/2T)} \\ &\times \int \frac{d^2\mathbf{q}}{(2\pi)^2} \Gamma_y^{(1)}(\mathbf{q}, \omega, B) \Gamma_y^{(2)}(\mathbf{q}, \omega, -B) |U(\mathbf{q}, \omega)|^2. \end{aligned} \quad (16)$$

A careful analysis shows that at low temperatures,  $T \ll \Gamma$ , the contribution of  $\Gamma^{(\Gamma/\hbar\omega_c)}$  to  $\rho^{(D)}$  dominates. Performing the remaining integrals yields the final result

$$\begin{aligned} \rho_{xx}^D &= \frac{8}{3\pi^2 e^2} \frac{1}{(k_F d)^2} \frac{1}{(\kappa R_c)^2} \left(\frac{T}{\Gamma}\right)^2 \ln\left(\frac{R_c \Gamma}{d\omega_c}\right) \\ &\times \left(\frac{E - E_N}{\Gamma}\right)^2 \left[ 1 - \frac{(E - E_N)^2}{\Gamma^2} \right]^2. \end{aligned} \quad (17)$$

for the drag resistivity of identical layers. Thus at low temperature  $T \ll \Gamma$ , the drag resistivity scales with magnetic field and temperature as

$$\rho_{xx}^D \propto T^2 B \ln B, \quad (18)$$

which compares nicely to the empirical scaling reported in Ref. [6],

$$\rho_{xx}^D \propto \left(\frac{n}{B}\right)^{-2.7} f(T/B), \quad (19)$$

with  $f(x) \sim x^2$ .

For different filling factors (or densities) in the two layers, the cyclotron radii of the two layers are no longer the same. If the cyclotron radii  $R_c$  of the



two layers are slightly different, such that  $\delta R_c/d \ll 1$ , the above calculation fully applies, and the result is obtained by the replacement

$$\begin{aligned} & \left( \frac{E - E_N}{\Gamma^2} \right)^2 \left[ 1 - \frac{(E - E_N)^2}{\Gamma^2} \right]^2 \\ & \rightarrow \left( \frac{E - E_N}{\Gamma} \left[ 1 - \frac{(E - E_N)^2}{\Gamma^2} \right] \right)_1 (\dots)_2 \end{aligned} \quad (20)$$

in Eq. (17). This yields an *oscillatory sign* of the drag resistivity. Importantly, for equal layer densities the drag resistivity is *positive*, in agreement with experiment. This result is different from the result for the diffusive regime discussed above [7]. The origin of the difference between the diffusive and the ballistic regime is that in the former (latter), the leading term originates from a longitudinal (transverse) contribution to  $\mathbf{\Gamma}$ .

If  $d \ll \delta R_c \ll R_c \Gamma / \omega_c$ , the calculation still applies if we make the replacement

$$\ln \left( \frac{R_c \Gamma}{d \omega_c} \right) \rightarrow \ln \left( \frac{R_c \Gamma}{\delta R_c \omega_c} \right) \quad (21)$$

of the logarithm in Eq. (17).

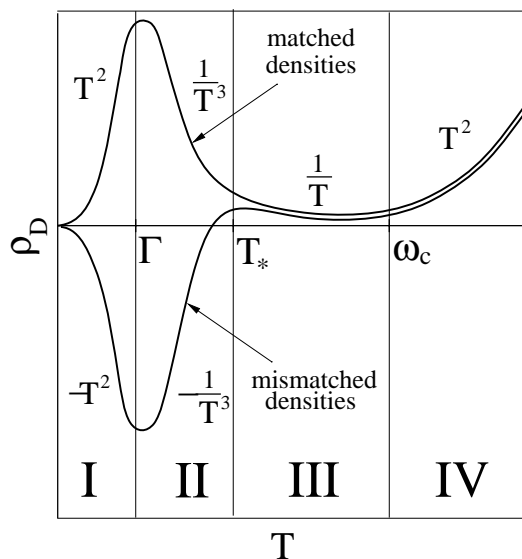


**Fig. 2.** Schematic temperature dependence of drag for matched and mismatched densities. In the latter case, the mismatch is chosen such that drag is negative at low temperatures.

For larger temperatures  $T \gg \Gamma$ , we find a number of different temperature regimes which are summarized in Fig. 2. For  $\Gamma \ll T \ll T_*$  (regime II in Fig. 2), we find that the drag resistivity scales as

$$\rho_{xx}^D \propto T^{-3} B^{7/2} \ln B \quad (22)$$

as function of  $B$  and  $T$ . This contribution arises from  $\Gamma^{(\Gamma/\hbar\omega_c)}$ . The upper limit of the temperature interval is given by

$$T_* \equiv \Gamma \left( \frac{\Gamma}{\omega_c} \right) k_F d. \quad (23)$$

For even higher temperatures, the conventional contribution  $\Gamma^{(q/k_F)}$  dominates and the drag resistivity becomes positive. Specifically, we find that the drag resistivity scales as

$$\rho_{xx}^D \propto T^{-1} B^{7/2} \quad (24)$$

for  $T_* \ll T \ll \omega_c$  (regime III in Fig. 2) and as

$$\rho_{xx}^D \sim \frac{1}{e^2} \frac{1}{(k_F a)^2} \frac{1}{(\kappa R_c)^2} \left( \frac{T}{E_F} \right)^2 \left( \frac{\omega_c}{\Gamma} \right) \propto T^2 B^{1/2}. \quad (25)$$

for even higher temperatures  $T \gg \omega_c$  (region IV in Fig. 2).

## 4 Summary and outlook

Experimental studies of drag in high Landau levels have given a number of surprises, including negative drag and a non-monotonous temperature dependence. Earlier theoretical work had led to some understanding of the possibility of sign changes of drag in this regime, but the detailed predictions for the sign did not agree with experiment. In this contribution, we sketch our results for Coulomb drag in high Landau levels, obtained in the framework of a diagrammatic calculation. Our calculation treats the interlayer interaction perturbatively and accounts for disorder in the self-consistent Born approximation which is expected to become exact in the limit of high Landau levels. Focusing on the ballistic regime for well-separated Landau levels, we find that there are two types of contributions to the triangle vertex entering the expression for the drag resistivity which are associated with different sources for a particle-hole asymmetry. At high temperatures, the contribution arising from the particle-hole asymmetry due to the zero-field electron dispersion dominates. This contribution is positive and increases with temperature. At lower temperatures, an anomalous contribution dominates which arises from the particle-hole asymmetry associated with the Landau level spectrum. This contribution changes sign in a way which is consistent with experimental observations. We close by mentioning that it would be interesting to apply the

approach outlined here to the fractional quantum Hall regime close to half filling of the lowest Landau level.

**Acknowledgments** – We thank J.G.S. Lok, K. von Klitzing, A. Khaetskii, and Ady Stern for useful discussions. One of us thanks the Weizmann Institute for hospitality during the preparation of this manuscript (supported by LSF grant HPRI-CT-2001-00114 and the Einstein Center). This work has been supported by the DFG-Schwerpunkt “Quanten-Hall-Systeme” (FvO, IVG, ADM), SFB 290 (FvO), as well as the “Junge Akademie” (FvO).

## References

1. T.J. Gramila, J.P. Eisenstein, A.H. MacDonald, L.N. Pfeiffer, and K.W. West, Phys. Rev. Lett. **66**, 1216 (1991).
2. U. Sivan, P.M. Solomon, and H. Shtrikman, Phys. Rev. Lett. **68**, 1196 (1992).
3. L.Zheng and A.H. MacDonald, Phys. Rev. B **48**, 8203 (1993).
4. X.G. Feng, S. Zelakiewicz, H. Noh, T.J. Ragucci, and T.J. Gramila, Phys. Rev. Lett. **81**, 3219 (1998).
5. J.G.S. Lok, S. Kraus, M. Pohl, W. Dietsche, K. von Klitzing, W. Wegscheider, and M. Bichler, Phys. Rev. B **63**, 041305 (2001).
6. K. Muraki, J.G.S. Lok, S. Kraus, W. Dietsche, K. von Klitzing, D. Schuh, M. Bichler, and W. Wegscheider, cond-mat/0311151 (2003).
7. F. von Oppen, S.H. Simon, and A. Stern, Phys. Rev. Lett. **87**, 106803 (2001).
8. I.V. Gornyi, A.D. Mirlin, and F. von Oppen, in preparation (2004).
9. M.C. Bønsager, K. Flensberg, B.Y. Hu, and A.-P. Jauho, Phys. Rev. B **56**, 10314 (1997).
10. K. Flensberg, B.Y. Hu, A.-P. Jauho, and J.M. Kinaret, Phys. Rev. B **52**, 14761 (1995).
11. A. Kamenev and Y. Oreg, Phys. Rev. B **52**, 7516 (1995).
12. B. N. Narozhny and I. L. Aleiner, and Ady Stern, Phys. Rev. Lett. **86**, 3610 (2001).
13. T. Ando and Y. Uemura, J. Phys. Soc. Jpn. **36**, 959 (1974); T. Ando, *ibid* **37**, 1233 (1974).
14. K.A. Benedict and J.C. Chalker, J. of Physics C **19**, 3587 (1986).
15. I.L. Aleiner and L. Glazman, Phys. Rev. B **52**, 11296 (1995).
16. A. Khaetskii and Yu. Nazarov, Phys. Rev. B **59**, 7551 (1999).